FUDMA Journal of Sciences (FJS)
ISSN online: 2616-1370
ISSN print: 2645 - 2944
Vol. 10 No. 24, December, 2026, pp 51 – 63
DOI: https://doi.org/10.33003/fjs-2026-1024-6596

GIS-Based Flood Susceptibility Mapping of Esan North-East Local Government Area, Edo State, Nigeria, using Remote Sensing and the Analytic Hierarchy Process

[1]Augustine Iyekeoretin Agbonaye, [1]Elimian Caleb Osejele and *[2]Stephen Olushola Oladosu

[1]Department of Civil Engineering, University of Benin, Benin City, Edo State, Nigeria.
[2]Department of Geomatics Engineering, University of Benin, Benin City, Edo State, Nigeria.

*Corresponding authors' email: olushola.oladosu@uniben.edu

Received: 05 Oct. 2026
Accepted: 20 Nov. 2026
Published: 23 Nov. 2026

ABSTRACT
Flood susceptibility mapping identifies areas whose physical and environmental characteristics make them more prone to flooding. This study assessed the relative physical flood susceptibility of Esan North-East Local Government Area, Edo State, Nigeria, using remote sensing, geographic information systems (GIS), the Analytical Hierarchy Process (AHP) and weighted overlay analysis. Six conditioning factors were considered: elevation, slope, precipitation, land use/land cover (LULC), drainage density and soil type. The thematic layers were prepared, reclassified into five susceptibility ratings and assigned relative weights through pairwise comparisons using the AHP framework. The resulting weights showed that slope (27.18%), elevation (25.51%) and precipitation (25.38%) had the highest relative importance, jointly accounting for 78.07% of the total weight. The pairwise comparison matrix produced a consistency ratio of 0.0242, indicating an acceptable level of consistency. The weighted overlay generated a flood susceptibility map that classified the study area into low, moderate and high susceptibility zones. The resulting map provides spatial information for preliminary land-use screening and the identification of locations requiring further hydrological investigation and flood-management attention. However, the assessment represents relative physical susceptibility rather than observed flood extent, inundation depth or social vulnerability. Independent validation against a georeferenced flood inventory was not undertaken; therefore, the map should be interpreted as a preliminary decision-support product.

Keywords: Flood susceptibility, Geographic information systems, Remote sensing, Analytical Hierarchy Process, Weighted overlay, Esan North-East

INTRODUCTION

Flooding occurs when water accumulates on normally dry land following rainfall, river overflow, inadequate drainage or other processes that exceed the capacity of the local drainage system. The spatial distribution of flooding is influenced by meteorological conditions and the physical characteristics of a catchment. Rainfall supplies water to the system, while elevation, slope, soil properties and drainage characteristics influence infiltration, storage and runoff. Land-use and land-cover conditions also affect the partitioning of rainfall between infiltration and surface runoff. Changes in climate and land use can therefore modify flood-generating processes (Hirabayashi *et al*., 2013; Sofia *et al*., 2017). In Nigeria, studies have identified intense rainfall, inadequate drainage, encroachment on waterways and other human activities among factors that contribute to flood impacts (Abolade *et al*., 2013; Agbonkhese et al., 2014; Komolafe *et al.,* 2015; Echendu, 2021).

National flood outlooks identify rainfall conditions, antecedent soil moisture, topography and dam operations as factors relevant to flood occurrence in Nigeria (Nigeria Hydrological Services Agency, 2020). These factors operate at different spatial and temporal scales. Rainfall represents the principal meteorological input, whereas topography, soil and drainage influence the movement and accumulation of surface water. Land-cover conditions can further modify infiltration and runoff. A spatial assessment that integrates these factors can therefore provide a more complete representation of relative flood susceptibility than an assessment based on a single variable.

GIS-based multi-criteria decision analysis is commonly used to combine spatial factors in flood-susceptibility mapping. The analytical hierarchy process (AHP) provides a structured approach for assigning relative importance to criteria through pairwise comparisons, while weighted overlay integrates the criterion weights with classified spatial layers. AHP and related approaches have been applied in different settings, including the Sundarban region of India and flood-prone areas in Ethiopia (Ali *et al*., 2019; Edamo et al., 2022). Comparative studies have also evaluated multi-criteria decision methods alongside machine-learning techniques (Khosravi *et al.*, 2019). The findings from these studies demonstrate the usefulness of spatial multi-criteria analysis, although criterion weights and classification thresholds remain dependent on local environmental conditions and the judgement framework adopted.

Major flood events in Nigeria, including those reported in 2012 and 2018, have affected settlements, livelihoods and infrastructure (National Emergency Management Agency, 2013; European Commission Joint Research Centre, 2018). National and regional reports establish the significance of flooding but do not describe the local distribution of physical susceptibility within Esan North-East. A local-scale assessment therefore requires spatially explicit conditioning information and a transparent method for integrating the selected factors.

Flood susceptibility, flood hazard, vulnerability and risk describe related but distinct aspects of flooding. Flood susceptibility refers to the relative propensity of locations to experience flooding based on their physical and environmental characteristics. Flood hazard additionally describes the probability and characteristics of a flood event, such as its extent, depth and duration. Vulnerability concerns the potential for people or assets to suffer harm, while risk reflects the interaction of hazard, exposure and vulnerability. This study evaluates physical flood susceptibility and does not estimate social vulnerability, population exposure, damage or flood risk.

The interpretation of an AHP-based susceptibility map depends on the quality and spatial resolution of the input datasets, the classification of the conditioning factors and the internal consistency of the pairwise comparisons. AHP consistency statistics measure the coherence of the decision matrix; they do not constitute independent validation of the resulting map. Independent validation requires comparison with observed flood locations or a dated flood inventory. Where such observations are unavailable, the map should be interpreted as a relative susceptibility assessment rather than a validated representation of historical inundation.

The aim of this study was to map the relative physical flood susceptibility of Esan North-East Local Government Area, Edo State, by integrating elevation, slope, precipitation, LULC, drainage density and soil type through remote sensing, GIS, AHP and weighted overlay analysis.

MATERIALS AND METHODS

Study Area

Esan North-East Local Government Area is situated in Edo State, southern Nigeria, and its administrative headquarters is Uromi. The geographical centre of Esan North-East Local Government Area, Edo State, Nigeria, is located at approximately 6.8247° N latitude and 6.4578° E longitude, equivalent to 6° 49′ 29″ N and 6° 27′ 28″ E, respectively. These coordinates provide a central reference point for the study area and its spatial analysis. The study area covers approximately 338 km² and had a reported population estimate of 119,346. The area experiences a tropical seasonal rainfall regime, with the main rainy period occurring broadly between April and July and a shorter rainy period later in the year. The dry season generally extends from December to March. The study area and its location within Edo State are presented in Figure 1.

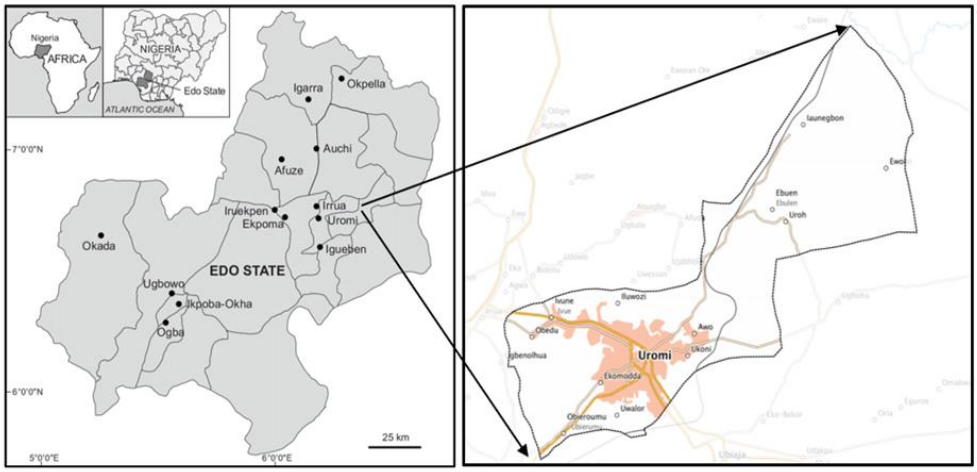


Figure 1: Location of Esan North-East Local Government Area in Edo State, Nigeria. Modified from (Nosazeogie et al., 2018)

Data Sources and Preparation

Six spatial conditioning factors were used in the assessment: elevation, slope, precipitation, LULC, drainage density and soil type. The datasets and sources reported for the analysis are summarised in Table 1. Landsat 8 imagery and Shuttle Radar Topography Mission (SRTM) elevation data were obtained from the United States Geological Survey (USGS). Topographic and geological information was obtained from the Federal Survey and the Nigerian Geological Survey Agency, respectively. Soil information was obtained from the Food and Agriculture Organization (FAO), while the rainfall dataset comprised 40 years of annual data ending in 2022.

Table 1: Spatial Datasets used in the Flood-Susceptibility Assessment

S/N	Data / Scale	Type	Source /Date
1.	Landsat 8 Satellite imagery (30m Resolution)	Remotely sensed	USGS (2022)
2.	SRTM Data (30m DEM Resolution)	Remotely sensed	USGS (2022)
3.	Topographical map 1:100,000	Digital Copy	Federal Survey (2018)
4.	Geological Map (1:500,000)	Digital copy	Nigerian Geological survey Agency (2018)
5.	FAO Soil Data	Remotely Sensed	FAO (2022)
6.	Rainfall Data	40 years Annual Data	1982 – 2022

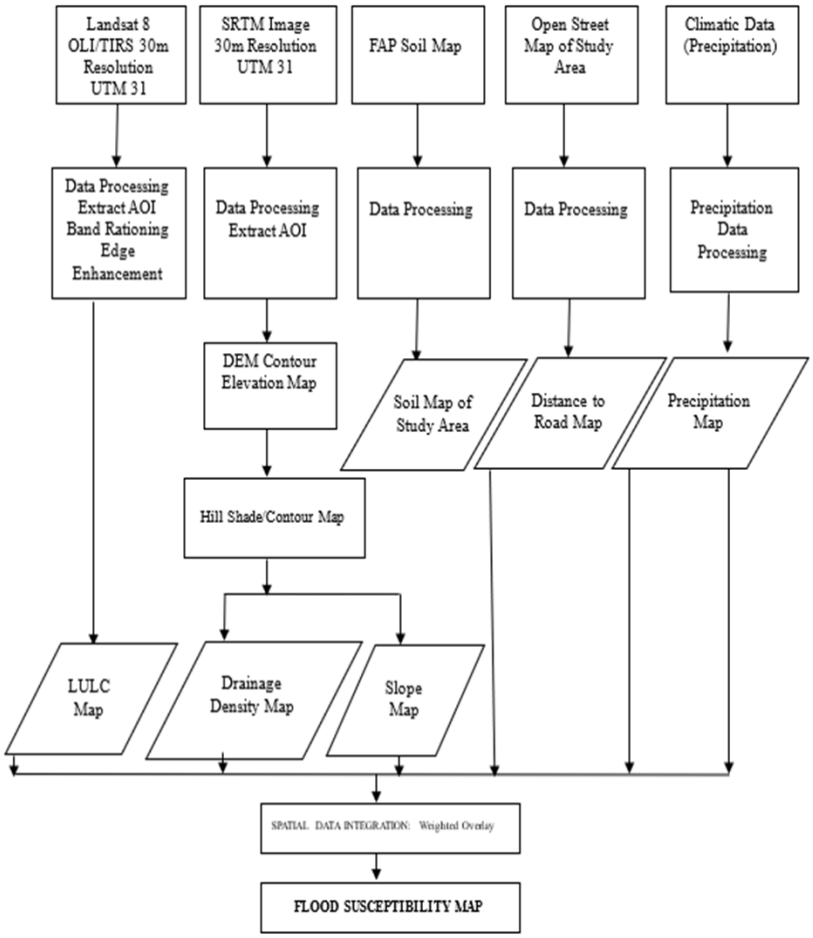


Figure 2: Layout for the preparation of flood susceptibility map

Data Acquisition

The spatial datasets were obtained from the providers listed in Table 1 and prepared for analysis within the study-area boundary.

Landsat imagery and land-use/land-cover mapping

Landsat 8 satellite imagery with a spatial resolution of 30 m was obtained from the USGS and used to prepare the land-use/land-cover layer. The LULC classes represented in the study were water body, built-up area, barren land and vegetation. The classified layer was reclassified according to the susceptibility ratings presented in Table 3.

Digital elevation model**:** Elevation data were obtained from the Shuttle Radar Topography Mission (SRTM) through the USGS EarthExplorer portal. The elevation model has a spatial resolution of 30 m and was used to derive slope and other terrain information.

Topographic, geological and soil information**:** Topographic information was obtained from the Federal Survey topographic map at a scale of 1:100,000. Geological information was obtained from the Nigerian Geological Survey Agency geological map at a scale of 1:500,000. The SRTM elevation model provided the basis for deriving terrain variables, while the thematic maps supplied the corresponding spatial information for the study area.

Soil data**:** Soil information was obtained from the FAO soil database. The soil classes represented in the study included silty clay, silty sediments and sandy clay. These soil classes were assigned susceptibility ratings based on their relative influence on infiltration and surface runoff.

Spatial Data Processing

i. The spatial datasets were prepared in WGS 84 / UTM Zone 31N. The thematic layers were clipped to the Esan North-East study boundary and prepared for integration in the GIS environment. Categorical layers were retained as discrete classes during resampling, while continuous terrain and rainfall data were treated as continuous surfaces. The common analysis extent was defined by the study-area boundary.
ii. The topographic and thematic maps used in the analysis were scanned and georeferenced to WGS 84 / UTM Zone 31N before digitisation and spatial processing.
iii. All input layers were clipped to the study-area boundary to provide a common spatial extent for the overlay analysis. The conditioning layers were converted to raster format and prepared for combination in the weighted-overlay procedure.

GIS Analysis

PCI Geomatica version 16 and ArcGIS 10.6.1 were used for spatial data preparation, terrain analysis, thematic mapping and overlay operations.

Terrain and Drainage Analysis

i. The SRTM elevation model was clipped to the study boundary and used to derive slope and hillshade layers. Contours were generated from the elevation model to support the interpretation of terrain variation. The resulting terrain information was used

in the preparation of the elevation and slope conditioning layers.

ii. Hard-copy thematic maps were scanned and georeferenced to WGS 84 / UTM Zone 31N before the relevant features were digitised for spatial analysis.

The Esan North-East administrative boundary defined the area of interest for clipping and processing the input datasets.

Drainage Density

i. The 30 m SRTM elevation model was used as the elevation source for terrain analysis and the preparation of the drainage-related layers.

ii. Contour lines were generated from the SRTM elevation model in ArcGIS and used to represent the spatial pattern of terrain elevation.

iii. Drainage lines were digitised from the terrain representation and used to derive the drainage-density layer. Drainage density expresses the total length of drainage channels per unit area and is conventionally reported in km/km² (equivalent to km^{-1}). The drainage-density values were classified into five susceptibility categories as presented in Table 3.

iv. The elevation, slope, contour and drainage layers were prepared in ArcGIS and incorporated into the flood-susceptibility modelling framework.

Flood-Susceptibility Modelling

Flood-susceptibility modelling was undertaken by integrating the six selected conditioning factors: elevation, slope, precipitation, LULC, drainage density and soil type. Each factor was represented as a spatial layer, reclassified into susceptibility ratings and assigned a relative weight through AHP. The weighted layers were then combined to produce a continuous flood-susceptibility index, which was grouped into low, moderate and high susceptibility classes.

1. Selection of conditioning factors
2. Each conditioning factor was divided into ordinal classes and assigned a susceptibility rating from 1 to 5, with higher values representing greater relative susceptibility. The class ranges and ratings used for elevation, slope, precipitation, LULC, drainage density and soil type are presented in Tables 2 and 3.
3. Pairwise comparison of the six criteria
4. The relative importance of the six criteria was evaluated using the Saaty fundamental scale. The pairwise comparison matrix was constructed as a reciprocal matrix, such that the comparison of criterion i with criterion j is the reciprocal of the comparison of criterion j with criterion i. The matrix entries and the corresponding normalized weights are presented in Table 6 and Table 7.
5. Derivation of criterion weights
6. The normalized priority vector was derived from the principal eigenvector of the reciprocal pairwise comparison matrix. The resulting weights were normalized so that their sum equalled one and were applied as the criterion weights in the weighted-overlay analysis.

Reclassification of Conditioning Factors

The six conditioning factors were reclassified into five susceptibility ratings. Elevation and slope were classified according to their ranges in the study area. Precipitation was grouped into five classes based on the rainfall surface used in the analysis. LULC classes were assigned ratings according to their expected influence on infiltration and runoff. Drainage density and soil type were similarly reclassified to represent their relative contribution to surface-water accumulation and infiltration. The class ranges and ratings are shown in Tables 2 and 3.

Table 2: Flood-Conditioning Criteria and Susceptibility Ratings (Terrain and Precipitation Factors)

Flood Causative Criterion	Unit	Class Ranges and Rating	Susceptibility Class	Susceptibility Class Rating	Weight (%)
Elevation	m	-1–53	Very High	5	25.51
		54–91	High	4	
		92–131	Moderate	3	
		132–194	Low	2	
		195–306	Very Low	1	
Slope	%	< 2.15	Very High	5	27.18
		2.16–4.15	High	4	
		4.16–6.59	Moderate	3	
		6.60–10.46	Low	2	
		10.47–36.52	Very Low	1	
Precipitation	mm/yr	< 8.59	Very Low	1	25.38
		8.60–9.28	Low	2	
		9.29–10.03	Moderate	3	
		10.04–10.74	High	4	
		10.77–11.83	Very High	5	
Total					**78.07**

Table 3: Flood-Conditioning Criteria and Susceptibility Ratings (LULC, Drainage Density and Soil Factors)

Flood Causative Criterion	Unit	Class Ranges and Rating	Susceptibility Class	Susceptibility Class Rating	Weight (%)
LULC	Categorical	Water Body	Very High	5	10.29
		Built up Area	Moderate	3	
		Barren Land	Low	2	
		Vegetation	Very Low	1	
Drainage Density	km/km²	< 0.733	Very Low	1	6.11
		0.734–1.316	Low	2	
		1.317–1.917	Moderate	3	
		1.918–2.707	High	4	
		2.708–4.793	Very High	5	
Soil Type	Categorical	Silty Clay	Very High	5	5.53
		Silty Sediments	Moderate	3	
		Sandy Clay Sand	Low	2	
Total					**21.93**
Overall total					**100.00**

AHP Criterion Weighting

AHP was used to estimate the relative weights of elevation, slope, precipitation, LULC, drainage density and soil type. The pairwise comparison matrix was constructed using the relative-importance judgements reported in the original matrix. The normalized weights represent the decision priorities assigned to the six criteria and were used in the weighted-overlay calculation.

Table 4: Criteria and Sub-Criteria used in the AHP Framework

Criteria	Sub-Criteria for Elevation	Sub-Criteria for Slope	Sub-Criteria for Precipitation	Sub-Criteria for LULC	Sub-Criteria for Drainage Density	Sub-Criteria for Soil
Elevation	Slope	Elevation	Elevation	Elevation	Elevation	Elevation
Slope	Precipitation	Precipitation	Slope	Slope	Slope	Slope
Precipitation	LULC	LULC	LULC	Precipitation	Precipitation	Precipitation
LULC	Drainage Density	Drainage Density	Drainage Density	Drainage Density	LULC	LULC
Drainage Density	Soil Type	Soil Type	Soil Type	Soil Type	Soil Type	Drainage Density
Soil Type						

Saaty Pairwise-Comparison Scale

The relative importance of each pair of criteria was expressed using the fundamental 1–9 scale attributed to Saaty. A value of 1 indicates equal importance; 3, 5, 7 and 9 indicate progressively stronger preference; and 2, 4, 6 and 8 represent intermediate judgements. Reciprocal values express the reverse comparison.

Table 5: Saaty Scale for Pairwise Comparisons

Pairwise comparison	Relative importance	Numerical judgement
Elevation compared with Slope	Equal importance	1
Elevation compared with Precipitation	Equal importance	1
Elevation compared with LULC	Moderately greater importance	2
Elevation compared with Drainage density	Strongly greater importance	5
Elevation compared with Soil type	Strongly greater importance	5
Slope compared with Precipitation	Equal importance	1
Slope compared with LULC	Moderately greater importance	3
Slope compared with Drainage density	Strongly greater importance	5
Slope compared with Soil type	Strongly greater importance	5
Precipitation compared with LULC	Moderately greater importance	3
Precipitation compared with Drainage density	Strongly greater importance	5
Precipitation compared with Soil type	Moderately greater importance	3
LULC compared with Drainage density	Equal importance	1
LULC compared with Soil type	Moderately greater importance	3
Drainage density compared with Soil type	Equal importance	1

Sig. Strength	Explanation	Comments
1	Equal significance	Two elements contribute equally to the objective
3	Moderate significance	Judgment slightly favours one element over another
5	Strong significance	Judgment strongly favours one element over another
7	Very strong significance	Judgment strongly favours one element over another, its dominance is demonstrated by experience
9	Maximum significance	The dominance of one element over another is demonstrated and absolute
2, 4, 6, 8	Can be used to express intermediate values	

Pairwise Comparison Matrix

The reciprocal pairwise comparison matrix was constructed from the six-criterion judgements. The upper-triangular judgements in the reported matrix were retained, and the corresponding lower-triangular values were calculated as their mathematical reciprocals. This procedure ensures that $a_{ij} = 1/a_{ji}$ for every pair of criteria. The resulting matrix is presented in Table 6.

Table 6: Reciprocal Pairwise Comparison Matrix for the Six Flood-Conditioning Criteria

Criterion	Elevation	Slope	Precipitation	LULC	Drainage density	Soil type
Elevation	1	1	1	2	5	5
Slope	1	1	1	3	5	5
Precipitation	1	1	1	3	5	3
LULC	1/2	1/3	1/3	1	1	3
Drainage density	1/5	1/5	1/5	1	1	1
Soil type	1/5	1/5	1/3	1/3	1	1

Table 7: Normalized AHP Criterion Weights and Consistency Statistics

Criterion	Normalized weight	Weight (%)
Elevation	0.2551	25.51
Slope	0.2718	27.18
Precipitation	0.2538	25.38
LULC	0.1029	10.29
Drainage density	0.0611	6.11
Soil type	0.0554	5.54
Consistency statistics	λmax = 6.1502; CI = 0.0300	RI = 1.24; CR = 0.0242

Consistency Assessment

The consistency of the pairwise comparison matrix was evaluated using the consistency index (CI) and consistency ratio (CR). The principal eigenvalue, λmax, was obtained from the reciprocal matrix. For a matrix of order n, the consistency index is calculated using Equation 1:

$$CI = \frac{\lambda_{\max} - n}{n - 1} \quad (1)$$

The consistency ratio is calculated as follows using Equation 2:

$$CR = \frac{CI}{RI} \quad (2)$$

Where: CR is the consistency ratio, CI is the consistency index calculated from the pairwise comparison matrix, and RI is the random index corresponding to a matrix of the same size.

For six criteria, RI = 1.24. A CR below 0.10 indicates an acceptable level of consistency. The consistency statistics obtained from the reciprocal matrix are reported in Table 7.

Weighted-Overlay Generation

The final flood-susceptibility index was calculated using a weighted linear combination of the reclassified conditioning layers as shown in Equation 3:

$$FSI(x) = \sum_{i=1}^{n} w_i \, r_i(x) \quad (3)$$

Where: $FSI(x)$ is the susceptibility index at location x, w_i is the normalized Analytic Hierarchy Process weight for criterion i, $r_i(x)$ is the susceptibility rating of criterion i at location x, and n is the total number of criteria.

The six weighted layers were combined in the GIS to produce the final susceptibility surface, which was classified into low, moderate and high susceptibility zones.

The final map presents the spatial distribution of relative flood susceptibility within Esan North-East. The susceptibility classes indicate the relative influence of the selected physical conditioning factors and should not be interpreted as observed flood extent or measured inundation depth. Settlement-level interpretation is restricted to locations represented within the mapped study boundary.

RESULTS AND DISCUSSION

Spatial Distribution of Flood-Conditioning Factors

The six flood-conditioning factors selected for this study were mapped and reclassified before their integration through the AHP-weighted overlay. Figures 3–8 present the original thematic layers alongside their corresponding reclassified maps. The reclassification assigned relative susceptibility ratings to the different classes of each conditioning factor according to their expected influence on runoff generation, water movement and surface-water accumulation. These ratings represent the relative contribution of each class to the susceptibility model rather than direct observations of historical flood occurrence.

The selection of the six conditioning factors is consistent with previous flood-mapping investigations in Nigeria. Abubakar *et al.* (2025) applied GIS and AHP to integrate environmental

and hydro-geomorphological factors in flood-risk mapping of the Hadejia River Basin. Similarly, Ajibade *et al*. (2021) applied GIS-based AHP and fuzzy AHP to assess flood-prone areas in Ibadan using geomorphological characteristics. These studies demonstrate the relevance of combining multiple physical and environmental variables to examine spatial differences in flood susceptibility.

Slope

Slope was classified into five intervals: less than 2.15%, 2.16–4.15%, 4.16–6.59%, 6.60–10.46% and 10.47–36.52%. The respective susceptibility ratings were 5, 4, 3, 2 and 1. The classification assigns higher susceptibility ratings to areas with gentler slopes and lower ratings to steeper terrain. This reflects the potential for relatively flat surfaces to encourage slower surface-water movement and local accumulation, particularly where drainage capacity is limited.

The relationship between terrain gradient and flood susceptibility is also reflected in the work of Abubakar *et al.* (2025), who incorporated slope into their GIS-AHP flood-risk assessment of the Hadejia River Basin. Ajibade *et al*. (2021) similarly considered geomorphological characteristics in their GIS-based flood-prone area mapping of Ibadan. These studies support the consideration of slope as an important terrain-related variable in flood assessment. However, slope does not operate independently of other conditions, since rainfall intensity, soil infiltration properties and drainage characteristics also influence the movement and accumulation of surface water. Figure 3 presents the original slope surface and its reclassified layer.

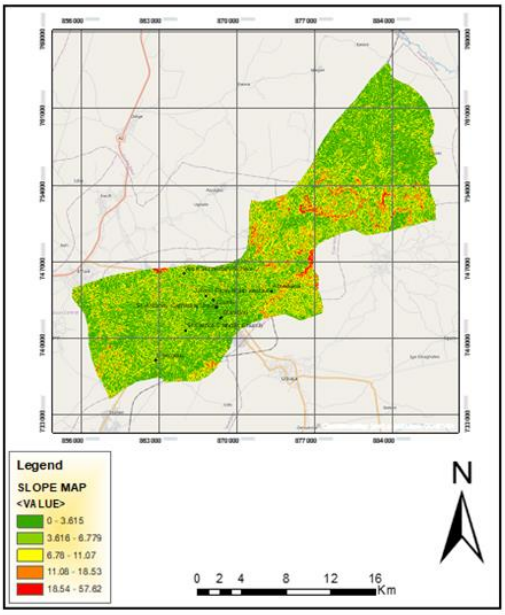


Figure 3 (a) Esan North East Slope Map

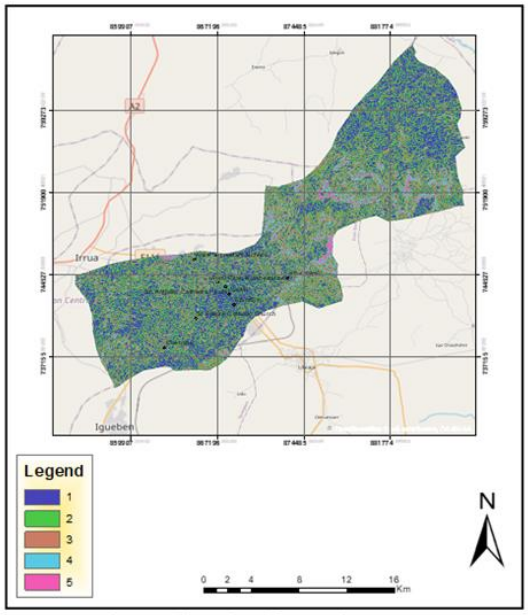


Figure 3 (b) Reclassify East Slope Map

Drainage Density

The drainage-density layer was classified into five intervals: less than 0.733, 0.734–1.316, 1.317–1.917, 1.918–2.707 and 2.708–4.793, with corresponding susceptibility ratings of 1, 2, 3, 4 and 5, respectively. Under this classification, areas with higher drainage density receive higher susceptibility ratings, reflecting the potential influence of concentrated drainage networks on runoff movement and the conveyance of surface water.

Drainage characteristics are relevant to flood assessment because the arrangement and capacity of drainage networks influence how runoff is collected and transported through a catchment. Yunus (2021), in a geospatial assessment of urban flood-risk areas, used a digital elevation model to derive flow direction and flow accumulation and subsequently delineated areas with different levels of flood exposure. Although the study did not employ the same AHP approach used in the present research, it demonstrates the value of terrain-derived drainage information in identifying locations that may be affected by surface-water accumulation. Abubakar *et al.* (2025) also incorporated drainage-related characteristics into their GIS-AHP flood-risk assessment. Figure 4 presents the mapped drainage-density distribution and its reclassified form.

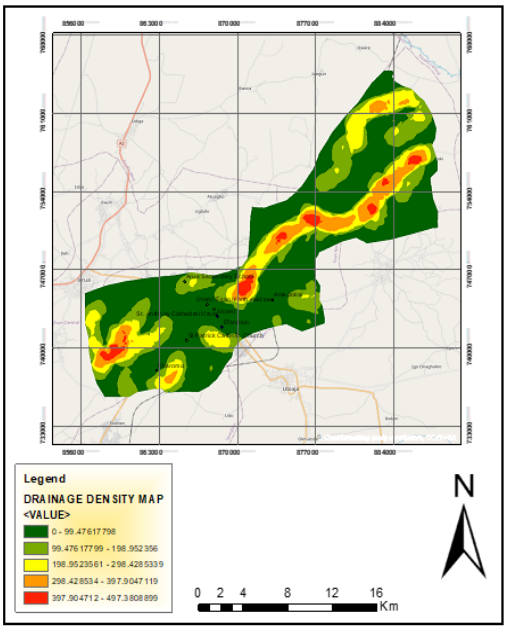


Figure 4 (a) Esan North East Drainage Density Map

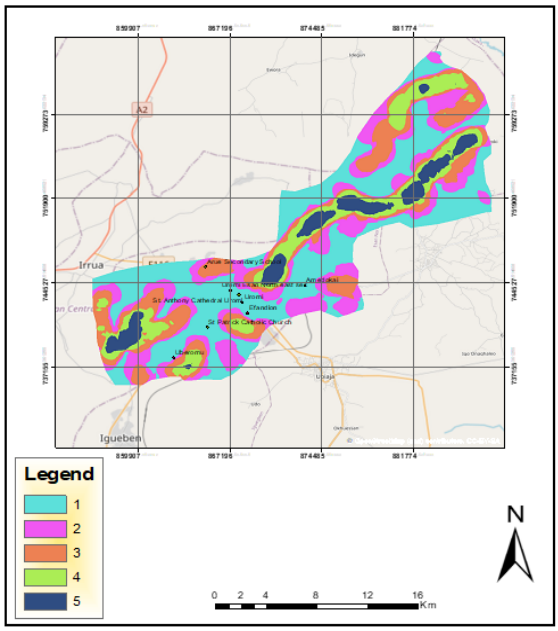


Figure 4(b) Reclassify Drainage Density Map

Elevation

Elevation was grouped into five intervals: −1–53 m, 54–91 m, 92–131 m, 132–194 m and 195–306 m. The assigned susceptibility ratings were 5, 4, 3, 2 and 1, respectively. The adopted classification therefore assigns higher susceptibility ratings to lower-lying terrain, reflecting its potential to receive and accumulate runoff from surrounding elevated locations.

The importance of elevation in flood assessment is demonstrated by Oyatayo *et al*. (2021), who integrated a digital elevation model, land-use/land-cover information and flood-frequency analysis to estimate potential inundation along the River Benue at Makurdi. Their results showed variations in the extent of inundation across different land-use categories under different flood return periods. Abubakar *et al.* (2025) also included elevation in their GIS-AHP assessment of the Hadejia River Basin. These studies support the inclusion of elevation as an important conditioning factor in the present assessment because terrain position influences the spatial movement and accumulation of surface water. Figure 5 presents the elevation model and its corresponding reclassified layer.

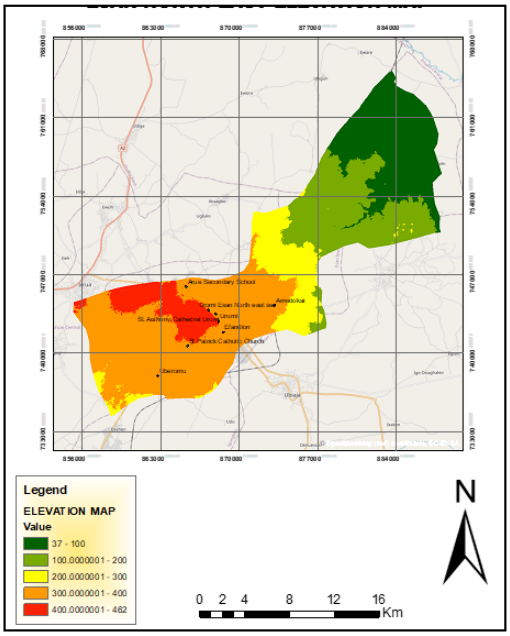


Figure (a) Esan North East Elevation Map

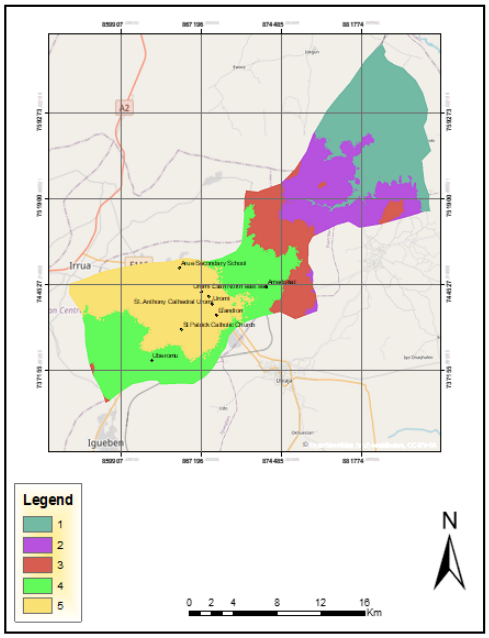


Figure 5 (b) Reclassify Elevation Map

Precipitation

The precipitation layer was classified into five intervals: less than 8.59, 8.60–9.28, 9.29–10.03, 10.04–10.74 and 10.77–11.83 mm/yr. The respective susceptibility ratings were 1, 2, 3, 4 and 5. The classification assigns higher susceptibility ratings to areas within the higher precipitation classes, reflecting the contribution of rainfall to runoff generation and potential flooding.

The relevance of precipitation to flood susceptibility is supported by Abubakar *et al.* (2025), who incorporated rainfall among the environmental factors used in their GIS-AHP flood-risk assessment. Majeed *et al.* (2023) also demonstrated the relevance of integrating environmental conditioning factors in flash-flood susceptibility prediction using AHP and frequency-ratio methods. These studies reinforce the need to consider rainfall alongside terrain and surface characteristics when examining the spatial distribution of flood susceptibility. Figure 6 presents the precipitation surface and its reclassified layer.

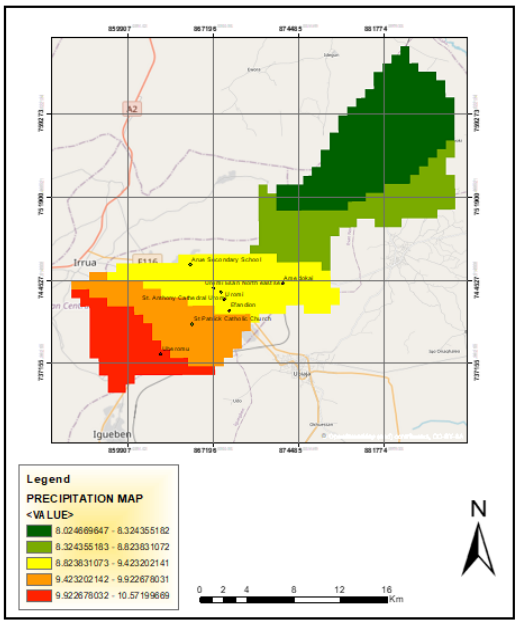


Figure 6 (a) Esan North East Precipitation

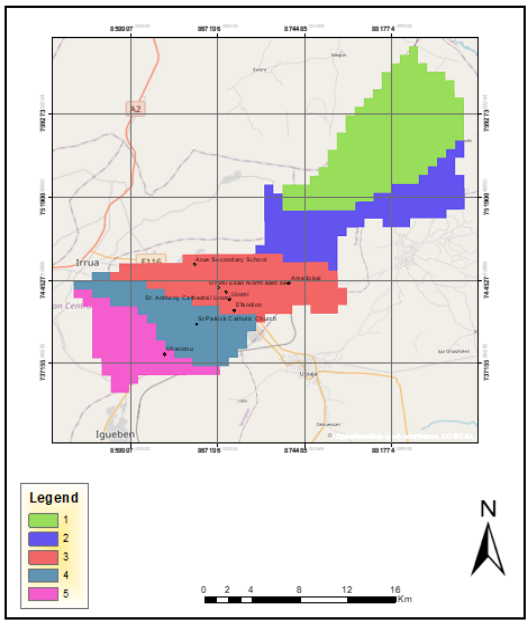


Figure 6 (b) Reclassify Precipitation Map

Soil Type

The soil-conditioning layer was incorporated to represent the potential influence of soil properties on infiltration and surface runoff. Differences in soil texture and composition can affect the rate at which rainfall infiltrates the ground and the proportion of water available for surface runoff. The original classification assigns a very high susceptibility rating to silty clay, a moderate rating to silty sediments and a low rating to sandy clay sand.

The inclusion of soil type is consistent with the approach adopted by Abubakar *et al.* (2025), who considered soil characteristics alongside terrain, rainfall and drainage-related variables in their GIS-AHP flood-risk assessment. Soil information provides an additional environmental dimension to the present assessment because differences in soil properties may influence the hydrological response of locations receiving similar rainfall. Figure 7 presents the original soil map and its reclassified layer.

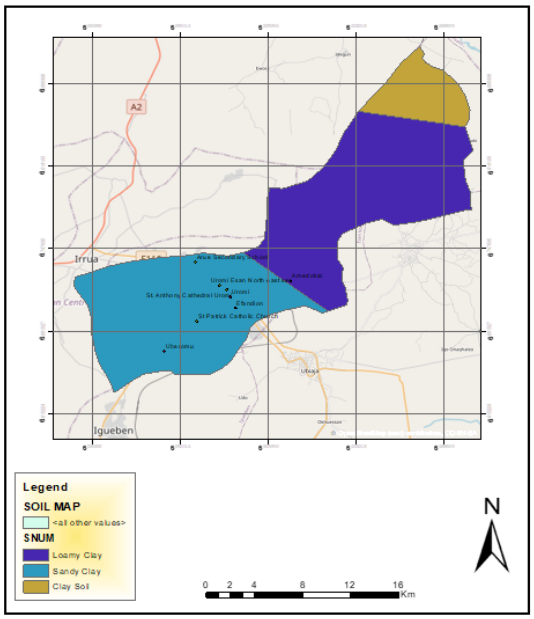


Figure 7 (a) Esan North East Soil Map

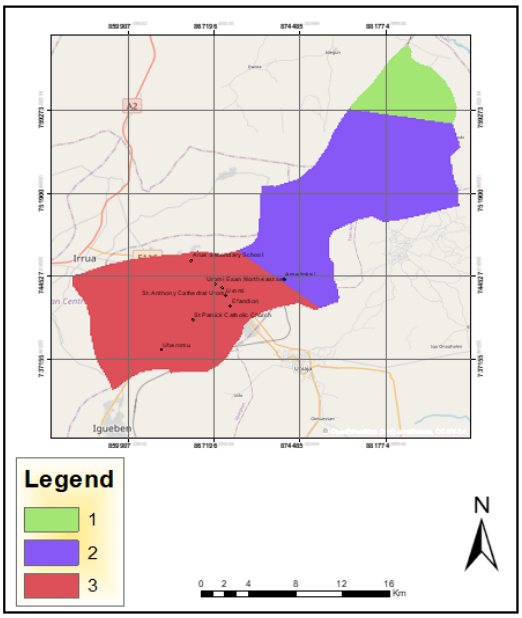


Figure 7(b) Reclassify Soil Map

Land Use/Land Cover

The land-use/land-cover layer was included because surface-cover characteristics influence infiltration, surface storage and runoff generation. The classification assigned susceptibility ratings of 5 to water bodies, 3 to built-up areas, 2 to barren land and 1 to vegetation. These ratings represent the relative susceptibility scheme adopted in the study, with water bodies receiving the highest rating and vegetation the lowest.

The importance of land-use/land-cover characteristics in flood assessment is demonstrated by Mukhtar *et al*. (2020), who examined land-use/land-cover changes and their effects on flooding in Kano Metropolis. Their results showed that built-up areas increased from 19.7% in 2001 to 34.4% in 2012, with a projected increase to 54.4% by 2035. Their hydrological modelling also indicated an increase in discharge in the Jakara Basin from 443 cm³/s in 2001 to 585.2 cm³/s in 2012 and a projected 609.7 cm³/s in 2035. These findings illustrate how changes in surface cover can influence runoff response and the hydrological behaviour of urban catchments.

Similarly, Oyatayo *et al.* (2021) integrated classified land-use/land-cover information with elevation and flood-frequency analysis to estimate the extent of inundation across different land-use categories along the River Benue at Makurdi. Their findings demonstrate the importance of considering land-cover characteristics when examining the spatial distribution of potentially inundated areas. These studies support the inclusion of LULC in the present assessment because the characteristics and distribution of surface cover influence the response of an area to rainfall and runoff. Figure 8 presents the original LULC map and its reclassified layer.

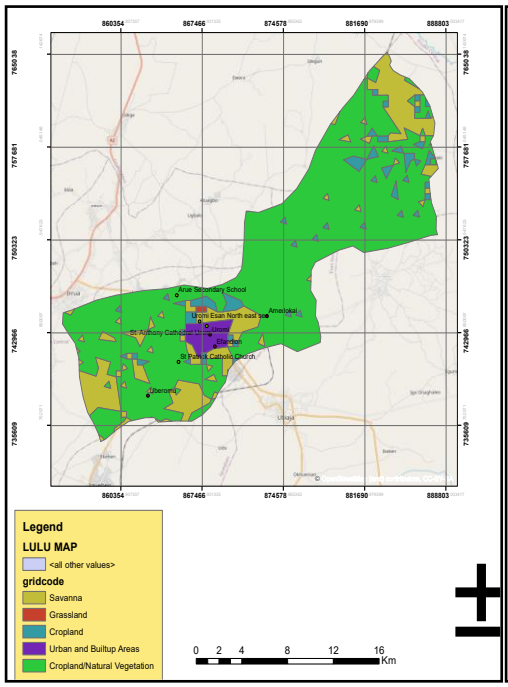


Figure 8 (a) Esan North East Lulc Map

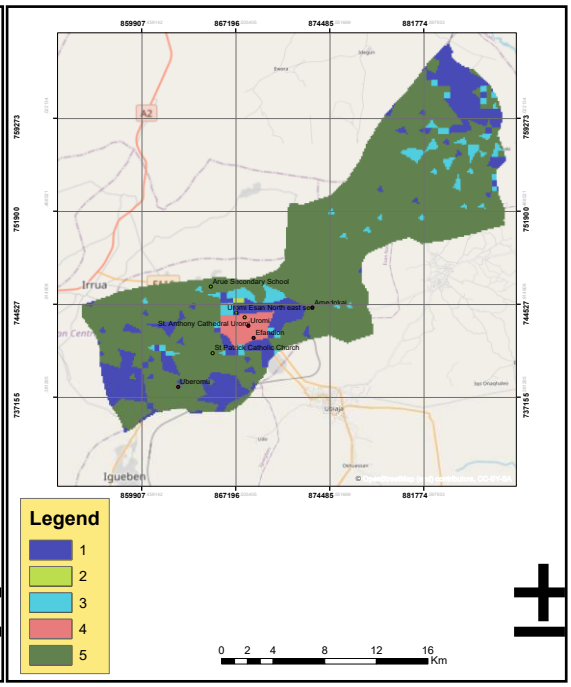


Figure 8(b) Reclassify Lulc Map

AHP Criterion Weights and Consistency

The normalized AHP weights obtained for the six flood-conditioning factors are presented in Table 7. Slope recorded the highest weight of 0.2718 (27.18%), followed by elevation at 0.2551 (25.51%) and precipitation at 0.2538 (25.38%). Land use/land cover contributed 0.1029 (10.29%), while drainage density and soil type recorded weights of 0.0611 (6.11%) and 0.0554 (5.54%), respectively.

The results indicate that slope, elevation and precipitation collectively account for approximately 78.07% of the total criterion weight. This shows that these three factors received greater relative importance within the pairwise comparison framework adopted for the study. The remaining criteria, comprising land use/land cover, drainage density and soil type, account for approximately 21.94% of the total weight based on the displayed normalized values. The resulting distribution reflects the priorities established through the AHP pairwise comparison process and should not be interpreted as an independent measurement of the actual physical contribution of each factor to flood occurrence.

The application of AHP for integrating multiple flood-conditioning factors is consistent with the work of Abubakar *et al*. (2025), who used GIS and AHP to assess flood susceptibility and vulnerability in the Hadejia River Basin. Ajibade *et al*. (2021) also applied AHP and fuzzy AHP to flood-prone area mapping in Ibadan. Their use of alternative analytical hierarchy frameworks demonstrates the suitability of multi-criteria decision analysis for integrating several environmental variables in flood mapping.

However, the relative importance assigned to individual factors may differ between study areas because of variations in environmental conditions, expert judgements and the criteria included in the pairwise comparison matrix. Khosravi *et al*. (2019), in their comparative assessment of multi-criteria decision-making and machine-learning methods, further demonstrated that flood susceptibility results can vary according to the modelling approach adopted. The weights obtained in the present study should therefore be understood as the relative priorities established through its own AHP framework rather than universal rankings applicable to other locations.

The consistency statistics obtained from the pairwise comparison matrix were $\lambda max = 6.1502$, consistency index (CI) = 0.0300, random index (RI) = 1.24 and consistency ratio

(CR) = 0.0242. The calculated consistency ratio is below the commonly accepted threshold of 0.10, indicating that the pairwise judgements satisfy the AHP consistency requirement. This suggests that the assigned relative preferences are sufficiently consistent for use in the weighted overlay. Nevertheless, the consistency ratio evaluates the internal consistency of the judgements; it does not constitute independent validation of the resulting flood susceptibility map.

Generation and Spatial Distribution of the Final Flood Susceptibility Map

Following the determination of the AHP criterion weights, the six reclassified conditioning factors were integrated using the weighted linear combination method to generate the final flood susceptibility index for Esan North-East Local Government Area. The overlay operation combined the spatial ratings of elevation, slope, precipitation, land use/land cover, drainage density and soil type according to their respective normalized weights. The resulting index represents the combined influence of the selected physical and environmental factors on the relative susceptibility of different locations to flooding.

The weighted integration gave greater relative influence to slope, elevation and precipitation, which together accounted for approximately 78.07% of the total model weight. Land use/land cover, drainage density and soil type accounted for the remaining approximately 21.94%, based on the displayed normalized values. This weighting arrangement means that the final susceptibility index was influenced more strongly by the spatial distribution and reclassified values of the first three factors within the adopted AHP framework.

The use of GIS and AHP to integrate multiple environmental factors is consistent with the approach reported by Abubakar *et al*. (2025) in the Hadejia River Basin. Similarly, Ajibade *et al.* (2021) demonstrated how GIS-based AHP and fuzzy AHP can be used to classify flood-prone areas into different susceptibility categories. These studies provide methodological support for the weighted integration adopted in the present assessment, although their study areas, conditioning factors and classification procedures differ from those used in Esan North-East.

The final susceptibility index was classified into three categories: low, moderate and high susceptibility. Areas with higher index values represent locations where the combined ratings of the selected conditioning factors produce comparatively greater susceptibility, while areas with lower index values represent locations with comparatively lower susceptibility ratings.

The spatial distribution of these classes is presented in Figure 9. The map constitutes the principal output of the GIS-based AHP assessment and provides a spatial basis for identifying locations that may require further hydrological investigation and consideration in local flood-management planning.

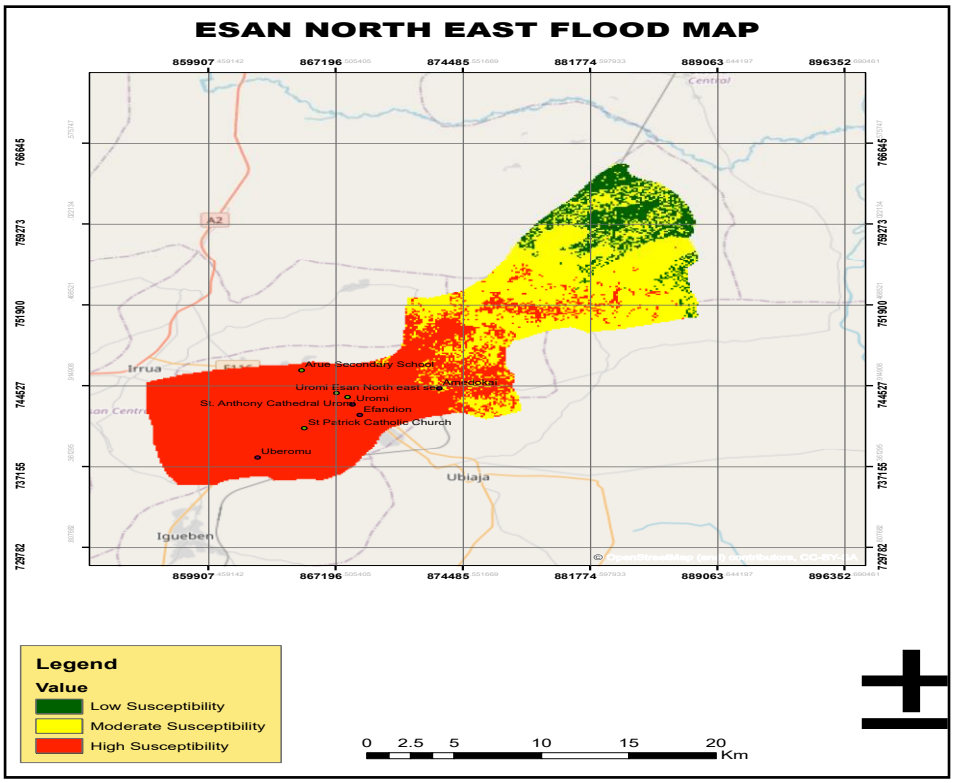


Figure 9: Final Flood Susceptibility Map of Esan North-East Local Government Area

The relevance of integrating terrain and land-cover information in flood mapping is also demonstrated by Oyatayo et al. (2021), whose Makurdi study combined digital elevation data, classified land use/land cover and flood-frequency analysis to estimate potential inundation under different flood return periods. Unlike that study, which incorporated observed river-stage and discharge records to estimate inundation under specified return periods, the present assessment produces a relative susceptibility map through AHP-weighted integration. The two approaches therefore provide complementary forms of flood assessment, but their outputs should not be interpreted as equivalent.

The final flood susceptibility map represents modelled physical susceptibility rather than observed flood occurrence, inundation depth or flood probability. Its interpretation is therefore limited by the quality and resolution of the input datasets, the selected conditioning factors, the classification thresholds and the subjective judgements involved in the

AHP weighting process. In addition, independent validation using historical flood locations or a suitable flood inventory was not undertaken. Consequently, the map should be interpreted as a preliminary spatial decision-support product for identifying relatively susceptible locations rather than as a validated prediction of actual flood extent.

CONCLUSION

This study integrated remote sensing, GIS, the analytical hierarchy process and weighted overlay to assess the relative physical flood susceptibility of Esan North-East Local Government Area, Edo State. Six conditioning factors: elevation, slope, precipitation, land use/land cover, drainage density and soil type, were incorporated into the analysis. The resulting map differentiates the study area into low, moderate and high relative susceptibility zones and provides spatial information that can support preliminary land-use screening and the prioritisation of locations for detailed hydrological investigation. The AHP comparison matrix was made reciprocal and its consistency was assessed using the consistency ratio. The mapped classes should be interpreted as relative susceptibility rather than observed flood extent, flood depth or social vulnerability. Independent validation against a georeferenced flood inventory was not undertaken; consequently, the map is best regarded as a preliminary decision-support product. Further work incorporating observed flood locations, field verification and detailed hydrological data would strengthen the assessment.

REFERENCES

Abolade O, Muili AB, Ikotun SA. (2013) Impacts of flood disaster in Agege Local Government Area, Lagos, Nigeria. International Journal of Development and Sustainability. 2 (4): 2354–2367.

Abubakar A, Sani M, Ahmad MH, Gambo J. (2025) Geospatial flood risk mapping and vulnerability assessment using GIS and AHP in Hadejia River Basin, Jigawa State, Nigeria. FUDMA Journal of Sciences. 9 (12): 793–804. https://doi.org/10.33003/fjs-2025-0912-4323

Adegboyega SA, Onuoha OC, Adesuji KA, Olajuyigbe AE, Olufemi AA, Ibitoye MO. (2018) An integrated approach to modelling of flood hazards in the rapidly growing city of Osogbo, Osun State, Nigeria. Space Science International. 4 (1): 1–15.

Aderogba KA. (2012) Global warming and challenges of floods in Lagos metropolis, Nigeria. Academic Research International. 2 (1): 455–468.

Agbonkhese O, Agbonkhese EG, Aka EO, Joe-Abaya J, Ocholi M, Adekunle A. (2014) Flood menace in Nigeria: Impacts, remedial and management strategies. Civil and Environmental Research. 6 (4): 32–40.

Ajibade FO, Ajibade TF, Idowu TE, Nwogwu NA, Adelodun B, Lasisi KH, Opafola OT, Ajala OA, Fadugba OG, Adewumi JR. (2021) Flood-prone area mapping using GIS-based analytical hierarchy frameworks for Ibadan city, Nigeria. Journal of Multi-Criteria Decision Analysis. 28 (5–6): 283–295. https://doi.org/10.1002/mcda.1759

Ali SA, Khatun R, Ahmad A, Ahmad SN. (2019) Application of GIS-based analytic hierarchy process and frequency ratio model to flood vulnerable mapping and risk area estimation at Sundarban region, India. Modeling Earth Systems and Environment. 5 (3): 1083–1102.

Echendu AJ. (2021) Flooding in Nigeria and Ghana: Opportunities for partnerships in disaster-risk reduction. Sustainability: Science, Practice and Policy. 18 (1): 1–15.

Edamo ML, Ukumo TY, Lohani TK, Ayana MT, Ayele MA, Mada ZM, Abdi DM. (2022) A comparative assessment of multi-criteria decision-making analysis and machine learning methods for flood susceptibility mapping and socio-economic impacts on flood risk in Abela-Abaya floodplain of Ethiopia. Environmental Challenges. 9: 100629. https://doi.org/10.1016/j.envc.2022.100629

European Commission Joint Research Centre. (2018) Update on floods in Nigeria. JRC Emergency Report No. 022. Available online at: https://reliefweb.int/sites/reliefweb.int/files/resources/2018-09-24_floods_nigeria_jrc_report.pdf (accessed 13 July 2020).

FAO Soils Portal. (2022) FAO Soils Portal.

Hirabayashi Y, Mahendran R, Koirala S, Konoshima L, Yamazaki D, Watanabe S, Kim H, Kanae S. (2013) Global flood risk under climate change. Nature Climate Change. 3: 816–821.

John-Nwagwu HO, Edith M, Hassan SH. (2014) Flood vulnerability assessment and disaster risk reduction in Kubwa, Federal Capital Territory, Nigeria. American Journal of Environmental Engineering and Science. 1 (2): 55–66.

Khosravi K, Shahabi H, Pham BT, Adamowski J, Shirzadi A, Pradhan B, Dou J, Ly HB, Gróf G, Ho HL, Hong H, Chapi K, Prakash I. (2019) A comparative assessment of flood susceptibility modeling using multi-criteria decision-making analysis and machine learning methods. Journal of Hydrology. 573: 311–323. https://doi.org/10.1016/j.jhydrol.2019.03.073

Khosravi K, Shahabi H, Pham BT, Adamowski J, Shirzadi A, Pradhan B, Dou J, Ly HB, Gróf G, Ho HL, Hong H, Chapi K, Prakash I. (2019) A comparative assessment of flood susceptibility modeling using multi-criteria decision-making analysis and machine learning methods. Journal of Hydrology. 573: 311–323. https://doi.org/10.1016/j.jhydrol.2019.03.073

Komolafe AA, Adegboyega SA, Akinluyi FO. (2015) A review of flood risk analysis in Nigeria. American Journal of Environmental Sciences. 11 (3): 157–166.

Majeed M, Lu L, Anwar MM, Tariq A, Qin S, El-Hefnawy M, El-Sharnouby M, Li Q, Alasmari A. (2023) Prediction of flash flood susceptibility using integrating analytic hierarchy process (AHP) and frequency ratio (FR) algorithms. Frontiers in Environmental Science. 10: 1037547. https://doi.org/10.3389/fenvs.2022.1037547

Mukhtar I, Iguisi EO, Shehu AU, Dabo Y, Abubakar M, Zubairu SM, Balarabe A. (2020) Effects of landuse and landcover change on flooding in Kano Metropolis, Kano State, Nigeria. FUDMA Journal of Sciences. 4 (3): 505–512. https://doi.org/10.33003/fjs-2020-0403-368

National Emergency Management Agency (NEMA). (2013) Report on flood disasters in Nigeria. Government Press, Abuja.

Nigeria Hydrological Services Agency. (2020) 2020 annual flood outlook. Available online at: https://nihsa.gov.ng/wp-content/uploads/2020/06/2020-NIHSA-Annual-Flood-Outlook-AFO-5-2.pdf (accessed 05 May 2024).

Nosazeogie E, Tende T, Monadjem A. (2018) Hooded vultures Necrosyrtes monachus nearly extirpated from Edo State, Nigeria: Report on the avian scavenger community. Ostrich. 89: 265–273. https://doi.org/10.2989/00306525.2018.1480069

Oyatayo KT, Ndabula C, Jeb DN, Adamu GK, Jidauna GG. (2021) Integrating digital elevation model, landuse/landcover and flood frequency analysis: A deterministic approach to flood inundation and risk modeling of Makurdi along its River Benue reach. FUDMA Journal of Sciences. 5 (1): 477–489. https://doi.org/10.33003/fjs-2021-0501-593

Sofia G, Roder G, Dalla Fontana G, Tarolli P. (2017) Flood dynamics in urbanized landscapes: 100 years of climate and human interaction. Scientific Reports. 7: 40527.

Umar N, Gray A. (2023) Flooding in Nigeria: A review of its occurrence and impacts and approaches to modelling flood data. International Journal of Environmental Studies. 80 (3): 540–561. https://doi.org/10.1080/00207233.2022.2081471

USGS EarthExplorer. Available online at: https://earthexplorer.usgs.gov/ (accessed 23 September 2021).

Yunus S. (2021) Delineation of urban flood risk areas using geospatial technique. FUDMA Journal of Sciences. 5 (1): 1–10. https://doi.org/10.33003/fjs-2021-0501-533

©2026 This is an Open Access article distributed under the terms of the Creative Commons Attribution 4.0 International license viewed via https://creativecommons.org/licenses/by/4.0/ which permits unrestricted use, distribution, and reproduction in any medium, provided the original work is cited appropriately.